Hydrol. Process. **22**, 2075–2085 (2008)
Published online 16 October 2007 in Wiley InterScience
(www.interscience.wiley.com) DOI: 10.1002/hyp.6807

Effect of growing watershed imperviousness on hydrograph parameters and peak discharge

Huang-jia Huang,[1] Shin-jen Cheng,[2]* Jet-chau Wen[3] and Ju-huang Lee[4]

[1] *Graduate School of Engineering Science and Technology, National Yunlin University of Science and Technology, Yunlin, Taiwan, ROC*
[2] *Department of Environment and Resources Engineering, Diwan University, Tainan, Taiwan, ROC*
[3] *Department of Safety Health and Environmental Engineering, National Yunlin University of Science and Technology, Yunlin, Taiwan, ROC*
[4] *Water Resources Agency, Ministry of Economic Affairs, Taipei, Taiwan, ROC*

Abstract:

An increasing impervious area is quickly extending over the Wu-Tu watershed due to the endless demands of the people. Generally, impervious paving is a major result of urbanization and more recently has had the potential to produce more enormous flood disasters than those of the past. In this study, 40 available rainfall–runoff events were chosen to calibrate the applicable parameters of the models and to determine the relationships between the impervious surfaces and the calibrated parameters. Model inputs came from the outcomes of the block kriging method and the non-linear programming method. In the optimal process, the shuffled complex evolution method and three criteria were applied to compare the observed and simulated hydrographs. The tendencies of the variations of the parameters with their corresponding imperviousness were established through regression analysis. Ten cases were used to examine the established equations of the parameters and impervious covers. Finally, the design flood routines of various return periods were furnished through use of approaches containing a design storm, block kriging, the SCS model, and a rainfall-runoff model with established functional relationships. These simulated flood hydrographs were used to compare and understand the past, present, and future hydrological conditions of the watershed studied. In the research results, the time to peak of flood hydrographs for various storms was diminished approximately from 11 h to 6 h in different decrements, whereas peak flow increased respectively from 127 m^3 s^{-1} to 629 m^3 s^{-1} for different storm intensities. In addition, this study provides a design diagram for the peak flow ratio to help engineers and designers to construct hydraulic structures efficiently and prevent possible damage to human life and property. Copyright © 2007 John Wiley & Sons, Ltd.

KEY WORDS block kriging; flood modelling; SCS; NLP; time to peak; peak flow

Received 16 October 2006; Accepted 1 May 2007

INTRODUCTION

In the hydrological cycle, precipitation falls onto the land surface. Some precipitation is intercepted or evaporated and some becomes surface, subsurface and groundwater runoff through the infiltration mechanism. Finally, all of the runoffs are collected into the streams or rivers, which then flow into the sea (Chow *et al.*, 1988). People mainly dwell in the downstream area of a basin, and tribal societies or cities often develop according to the living quality of the environment. The development of an urban area within a watershed causes a drastic change of land use and has major effects on the functioning of the hydrological status of that area during flood conditions (Simmons and Reynolds, 1982; Ferguson and Suckling, 1990; Leopold, 1991; Sala and Inbar, 1992; Singh, 1998; Gremillion *et al.*, 2000).

The ever-growing urban cities, with relatively scarce land and water resources, require proper planning for the enhancement of living conditions for the city dwellers. As the population concentration increases, the demand for land and water resources increases. Urbanization affects both quantity and quality of stormwater runoff. Planning for future public utilities requires incorporating these effects (Loganathan and Delleur, 1984; Driver and Troutman, 1989; Marsalek and Sztruhar, 1994; Tsihrintzis and Hamid, 1997). Hence, urban stormwater management has been one of the areas of active research in hydrology. Models describing stormwater management are varied in detail, depending upon the level of accuracy desired.

Hydrological modelling has often been used to simulate surface runoff by considering a watershed as an independent system (Clarke, 1973; Beven, 1989; Jin, 1992; Franchini and O'Connell, 1996; Melone *et al.*, 1998; Yue and Hashino, 2000; Hannah and Gurnell, 2001; Agirre *et al.*, 2005; Lee and Singh, 2005). Recently, systems analysis has been increasingly used as an aid in understanding and developing solutions to complex urban problems (Kang *et al.*, 1998; Cheng and Wang, 2002; Rodriguez *et al.*, 2003). Among the problems of urban stormwater management, systems analysis may be advantageously applied to determine the volume, flow rate and quality of urban storm runoff.

Reduced flow time and increments of both runoff volume and peak discharge are familiar problems of urban stormwater management (Changnon *et al.*, 1996;

* Correspondence to: Shin-jen Cheng, Department of Environment and Resources Engineering, Diwan University, 87-1, Nan-shih Li, Madou, 721, Tainan, Taiwan, ROC. E-mail: sjcheng@mail.dwu.edu.tw.

Krug, 1996; Bonta *et al*., 1997; Kang *et al*., 1998; Wong and Li, 1999; Cheng and Wang, 2002; Rodriguez *et al*., 2003). Simulation modelling and the design storm approach have been frequently used to estimate the magnitude and frequency of floods in urban areas, and to evaluate the hydrological effects on the characteristics of stormwater runoff with increasing impervious areas. These combined effects include increased runoff volume, reduced flow time, and an increase in peak discharges with a resulting shift in the flood frequency curve (Hollis, 1975; Moscrip and Montgomery, 1997; Moon *et al*., 2004).

WATERSHED DESCRIPTION

Area feature

The upstream Wu-Tu watershed was chosen to investigate the flood hydrographs undergoing urbanization for the research area of this case study. The watershed surrounds the city of Taipei in the north of Taiwan, as illustrated in Figure 1. The area of the Wu-Tu watershed is about 204 km^2, and the mean annual precipitation and runoff depth are 2865 mm and 2177 mm respectively. Owing to the rugged topography of the watershed, the runoff pathlines are short and steep, and the rainfall is non-uniform in both time and space. Large floods arrive rapidly in the middle to downstream reaches of the watershed, causing serious damage during summer.

Material studied

There are three rain-gauges (Jui-Fang, Wu-Tu and Huo-Shao-Liao) and one discharge site (Wu-Tu) on the Wu-Tu watershed, and available recordings of 50 rainfall–runoff events from 1966 to 2002 were used herein as the study sample. The annual data of population density and imperviousness percentages were used as urbanization degrees in the research area.

Usually, an impervious area is considered as a major cause of urbanization, and its definition is that in which all rainfall falling on the surface is presumed to produce surface runoff. The annual imperviousness percentage was computed according to this definition for streets, roads, railroad lines, highways, roofs, buildings, parking lots, ponds or lakes, waterways, and so on for each year. Table I lists the population intensity and percentages of impervious areas over the Wu-Tu watershed from 1966 to 2002, in which an obvious correlation exists between population and imperviousness. They can conveniently approximate the extent of urbanization and demonstrate the significance of the hydrological consequences of the ongoing urbanization of the Wu-Tu watershed.

Table I. The growth of population and imperviousness of the upstream Wu-Tu watershed

Year	Population intensity (km^{-2})	Impervious area (%)	Year	Population intensity (km^{-2})	Impervious area (%)
1966	385·01	4·78	1985	437·76	7·27
1967	390·54	5·02	1986	436·68	7·33
1968	398·78	5·10	1987	434·72	7·41
1969	407·20	5·18	1988	439·27	7·59
1970	413·84	5·26	1989	452·59	7·76
1971	417·49	5·34	1990	459·68	9·59
1972	419·68	5·42	1991	470·22	10·90
1973	418·58	5·50	1992	484·38	10·95
1974	420·29	5·57	1993	506·20	11·03
1975	419·86	5·65	1994	517·06	10·65
1976	422·20	5·73	1995	537·83	10·67
1977	424·16	5·83	1996	560·12	10·27
1978	419·79	5·95	1997	540·55	10·44
1979	418·75	6·12	1998	549·31	10·52
1980	426·46	6·54	1999	558·35	10·60
1981	433·01	6·80	2000	639·33	10·92
1982	438·36	6·99	2001	649·84	10·92
1983	436·00	7·12	2002	654·80	12·46
1984	437·74	7·19			

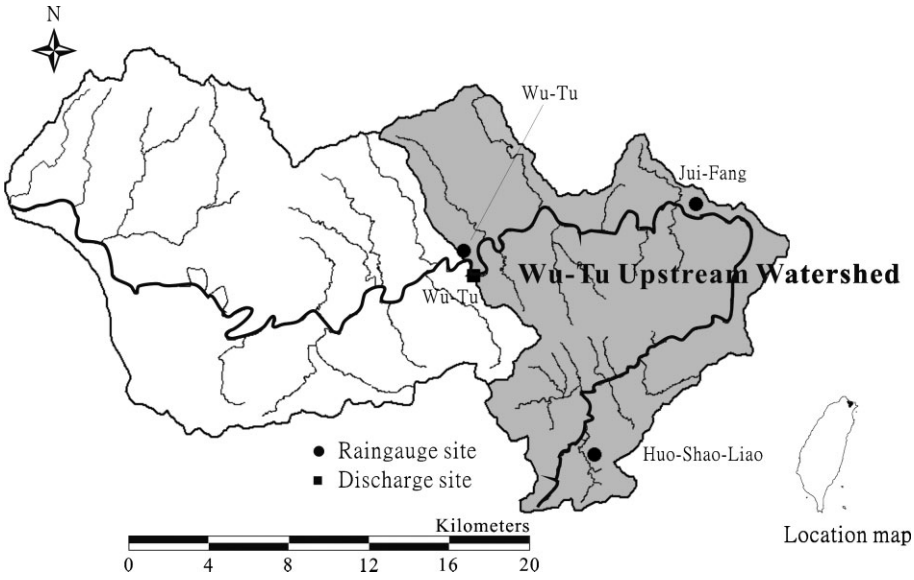

Figure 1. Location map and observed sites of the upstream Wu-Tu watershed

DOI: 10.1002/hyp

METHODS DESCRIPTIONS

Determining varied tendencies of parameters with their corresponding imperviousness is the major focus of this study. In order to achieve this objective, some popular methods were adopted herein, such as block kriging, non-linear programming, the SCS model, a lumped model, and a design storm. Three evaluated criteria were used to compare simulated hydrographs with actual observations. These simulated hydrographs of design floods were finally used to compare and understand the past, present, and future hydrological conditions of the watershed studied.

The block kriging method

Block kriging, which originally was developed by Matheron (1971) and has many applications in various research fields (Lebel and Bastin, 1985; Lebel *et al.*, 1987; Goovaerts, 2000; Syed *et al.*, 2003), was used herein to compute the mean rainfall.

In kriging, the optimal weightings λ_i are computed from the kriging system based on the Lagrange multipliers method (Wackernagel, 1998; Chiles and Delfiner, 1999), which are expressed as

$$\begin{cases} \sum_{j=1}^{n} \lambda_j \gamma(x_i, x_j) + \mu = \overline{\gamma}(V, x_i) \quad i = 1, 2, \ldots, n \\ \sum_{i=1}^{n} \lambda_i = 1 \end{cases} \tag{1}$$

$$\sigma_{\mathrm{K}}^2 = \sum_{i=1}^{n} \lambda_i \overline{\gamma}(V, x_i) + \mu \tag{2}$$

where $\gamma(x_i, x_j)$ is the semi-variogram of rain-gauges x_i and x_j(mm^2), $\overline{\gamma}(V, x_i)$ represents the average semi-variogram of the estimated area V and rain-gauge x_i (mm^2), σ_{K}^2 (mm^2) is the kriging estimated variance, and μ (mm^2) denotes the Lagrange multipliers.

For practical applications, Cheng and Wang (2002) established the basic semi-variogram on a project basin by using dimensionless rainfall data and then they described the detailed calculated procedure. The basic experimental semi-variogram is shown below:

$$\gamma(t, h_{ij}) = s^2(t)\gamma_{\mathrm{d}}^*(h_{ij}, a) \tag{3}$$

in which

$$\gamma_{\mathrm{d}}^*(h_{ij}, a) = \frac{1}{2T} \sum_{t=1}^{T} \left[\frac{p(t, x_i) - p(t, x_j)}{s(t)} \right]^2 \tag{4}$$

where $\gamma_{\mathrm{d}}^*(h_{ij}, a)$ (mm^2) denotes the climatological mean semi-variogram, which is time invariant, h_{ij} represents the distance between arbitrary rain-gauges x_i and x_j (m), a (m) is the range of the climatological mean semi-variogram, $p(t, x_i)$ (mm) represents the rainfall of rain-gauge x_i for time period t, T (h) is the total duration of all rainfall events, and $s(t)$ (mm) denotes the standard deviation of rainfall of all rain-gauges for time period t.

The estimator Z_{K}^* represents the hourly mean rainfall, which is a linear combination of n available point-rainfall recordings $Z(x_i)$ located at x_i and with weightings λ_i. The kriging estimator can be expressed as

$$Z_{\mathrm{K}}^* = \sum_{i=1}^{n} \lambda_i Z(x_i) \tag{5}$$

Non-linear programming

The non-linear programming (NLP) method has confirmed that the time-variant distribution of excess rainfall for a single event is obtainable and advantageous in acquiring appropriate hydrological parameters to illustrate the urbanization characteristics of specific watersheds (Cheng and Wang, 2002). It is unlike traditional methods, such as the Φ-index, which only obtains a time-invariant value of rainfall loss. Therefore, the NLP method was selected herein to calculate the excess amount of the hourly mean rainfall.

In the NLP method, the inputs and outputs are the hourly mean rainfall I_t and direct runoff Q_t of an event respectively. Non-negative constrains are decision variables include hourly rainfall losses H_t, unit hydrograph U_t, and estimated errors of both Z_t and V_t (i.e., $0 \le H_t \le l_t, Z_t \ge 0, V_t \ge 0, U_t \ge 0$) are all the decision variables. The objective function is composed of the minimized summation of estimated errors Z_t and V_t. The constraint equations are the discrete convolution integral of routing runoff; the volume of effective rainfall is equal to direct runoff, the volume of the unit hydrograph is one and other constraints are non-negative. Detailed expressions of the NLP method can be found in the presentation of Cheng and Wang (2002).

The SCS model

The range of curve numbers CN is confined between 0 and 100 (Chow *et al.*, 1988). A higher curve number implies that there is less potential watershed retention of stormwater and, consequently, a higher potential for runoff volume. The SCS model (Tsihrintzis and Hamid, 1997) applies the following equations to estimate the cumulative runoff depth based on the cumulative rainfall depth:

$$\begin{cases} \sum q_t = \dfrac{\left(\sum r_t - KS\right)^2}{\sum r_t + (1-K)S} & \sum r_t > KS \\ \sum q_t = 0 & \sum r_t \le KS \end{cases} \tag{6}$$

and

$$S = \frac{1000}{\mathrm{CN}} - 10 \tag{7}$$

where Σq_t is the cumulative runoff depth at time period t, Σr_t is the cumulative rainfall depth at time period t, S is the potential maximum retention or ultimate storage capacity of the soil, and CN is the curve number. The term $I_{\mathrm{a}} = KS$ represents the initial abstraction of rainfall by infiltration, surface storage, and interception. The value for K is typically taken as 0·2. All variable units are

DOI: 10.1002/hyp

depths in inches except for CN, which is dimensionless. The instantaneous runoff depth q_t (inches) and discharge Q_t (cfs) for a time period t are given by

$$q_t = \sum q_t - \sum q_{t-1} \tag{8}$$

$$Q_t = \alpha \frac{q_t}{\Delta t} A \tag{9}$$

where A (acre) is the watershed drainage area, Δt (h) denotes the time interval over a total duration, and α is a unit conversion factor.

The rainfall–runoff routing model

Generally, many conceptual models with parameters originate from the instantaneous unit hydrograph (IUH). These parameters with physical significances are easily used to observe the hydrological status of urbanized watersheds with increasing imperviousness. The general form of the IUH U_n from the nth linear reservoir owning different storage constants k_n with time period t can be expressed as (Hsieh and Wang, 1999)

$$U_n(t) = \int_0^t U_{n-1}(\tau) \frac{1}{k_n} e^{-(t-\tau)/k_n} d\tau = \begin{cases} \frac{1}{k_1} e^{-t/k_1} & n = 1 \\ \sum_{i=1}^{n} \frac{k_i^{n-2}}{\prod_{j=1, j\neq i}^{n} (k_i - k_j)} e^{-t/k_i} & n \geq 2 \end{cases} \tag{10}$$

The Nash model is a special case of the above expression for assuming the equivalent storage coefficient of cascade linear reservoirs. The IUH of n cascade linear reservoirs for one unit of effective rainfall (Nash, 1958) is

$$U(t) = \frac{1}{k\Gamma(n)} e^{-t/k} \left(\frac{t}{k}\right)^{n-1} \tag{11}$$

The design storm approach

A design storm is generally produced from the intensity–duration–frequency (IDF) curves or from other statistical means based on rainfall records. The alternating block method, instantaneous intensity method, and triangular hyetograph method are usually used to yield a reasonable design storm. The design storm is frequently coupled with the rational formula or a unit hydrograph method to simulate the design flood hydrograph for water resources planning. These approaches neglect the storage carryover effect that may exist in the drainage system by ignoring the time interval between storms (Chow *et al.*, 1988).

Evaluation criteria

This study adopted three criteria to evaluate the suitability of the rainfall–runoff model for the basin of interest. These criteria are coefficient of efficiency CE, the error of peak discharge, and the error of the time for peak to arrive. The first criterion was originally proposed by Nash and Sutcliffe (1970). It is now commonly used as a measure of model performance in hydrology (e.g. Nayak *et al.*, 2005). CE is identical to the familiar coefficient of determination R^2 for a linear regression analysis. Generally speaking, the value of CE is much less than that of R^2. It has been shown that CE is a much superior measure of goodness-of-fit for model validation purposes compared with the familiar R^2 or the coefficient of determination (Legates and McCabe, 1999).

Peak flow and time to peak are also important aspects of a flood hydrograph. Hence, differences of peak quantity and time to peak between observations and simulations were also simultaneously examined in this study. The error of peak discharge and the error of the time for peak to arrive have also often been used to examine modelling result (e.g. Chen *et al.*, 2003; Moramarco *et al.*, 2005). These criteria are as follows:

1. Coefficient of efficiency CE is defined as

$$\mathrm{CE} = 1 - \frac{\sum_{t=1}^{T} [Q_{\mathrm{est}}(t) - Q_{\mathrm{obs}}(t)]^2}{\sum_{t=1}^{T} [Q_{\mathrm{obs}}(t) - \overline{Q}_{\mathrm{obs}}(t)]^2} \tag{12}$$

   where $Q_{\mathrm{est}}(t)$ denotes the discharge of the simulated hydrograph for time period t, $Q_{\mathrm{obs}}(t)$ is the discharge of the observed hydrograph for time period t and $\overline{Q}_{\mathrm{obs}}(t)$ represents the average discharge of the observed hydrograph for time period t. The better the fit, the closer CE is to one. A negative value of CE means that model predictions are worse than predictions using a constant equal to the average observed value.
2. The error of peak discharge $\mathrm{EQ_p}$ (%) is defined as

$$\mathrm{EQ_p}(\%) = \frac{Q_{\mathrm{p,est}} - Q_{\mathrm{p,obs}}}{Q_{\mathrm{p,obs}}} \times 100 \tag{13}$$

   where $Q_{\mathrm{p,est}}$ is the peak discharge of the simulated hydrograph and $Q_{\mathrm{p,obs}}$ is the peak discharge of the observed hydrograph.
3. The error of the time for peak to arrive $\mathrm{ET_p}$ is defined as

$$\mathrm{ET_p} = T_{\mathrm{p,est}} - T_{\mathrm{p,obs}} \tag{14}$$

   where $T_{\mathrm{p,est}}$ denotes the time for the simulated hydrograph peak to arrive and $T_{\mathrm{p,obs}}$ represents the time required for the observed hydrograph peak to arrive.

RESULTS AND DISCUSSION

Analysing the design hydrographs of floods for various degrees of impervious covering is the major goal of this study. Therefore, storm simulations using the SCS method and the conceptual hydrological model were adopted herein. The functional relationships between impervious areas and parameters including the hydrological and the SCS models were established for understanding the growth status of urbanization. Finally, a useful

DOI: 10.1002/hyp

diagram of peak ratio with corresponding magnitudes of rainfall and imperviousness was drawn up to provide management and planning of relative water resources.

Hourly area rainfall

The set of the time sequence of discontinuous point-rainfall depths $p(t, x)$ can be considered as a realization of two-dimensional random fields. Considering n rain-gauges in a river basin, for every time period t, a realization $\pi(t)$ of the random n vector can be expressed as

$$\pi(t) = \{p(t, x_1), p(t, x_2), \ldots, p(t, x_n)\} \quad (15)$$

The hourly semi-variogram is a function of time period t, isotropy, and a time average form with non-zero and T time interval. The results of the climatological mean semi-variogram for the 50 selected rainfall events and the power form applied for fitting are shown below and in Figure 2:

$$\gamma_d^*(h_{ij}, a) = \omega_0 h^a = 0{\cdot}137h^{0{\cdot}209} \quad r^2 = 0{\cdot}834 \quad (16)$$

where ω_0 (mm^2) denotes the sill of the climatological mean semi-variogram. Variance $s^2(t)$ of a realization $\pi(t)$ for each time period t can be easily calculated from the hourly measurements of rainfall, and then the hourly semi-variograms of rainfall events can be directly calculated by using Equations (3) and (16).

Calibration for rainfall–runoff model

The direct runoffs of the 40 samples chosen for calibration were estimated by assuming a constant baseflow. The excess values of the hourly mean rainfall were completed through the NLP method. In the calibrated process, the hydrological parameters reflecting changing land use were obtained through the shuffled complex evolution optimal algorithm (Duan *et al*., 1993). A comparison of the simulated and observed runoff hydrographs by the above three criteria (CE, EQ_p, ET_p) is given in Table II;

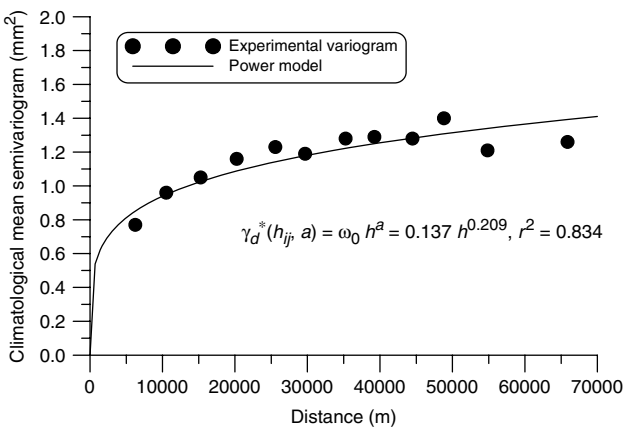

Figure 2. The climatological mean semi-variogram for the upstream Wu-Tu watershed

Table II. The calibrated results of the selected rainfall-runoff events

Event name (date)	CE	EQ_p	ET_p
Storm (20 Jun 1966)	0·951	−1·153	0
ALICE (2 Sep 1966)	0·912	−2·137	0
CORA (6 Sep 1966)	0·993	−0·943	0
ELSIE (13 Sep 1966)	0·969	−12·345	1
GILDA (16 Nov 1967)	0·980	−4·918	0
NADINE (26 Jul 1968)	0·988	−2·729	1
BETTY (7 Aug 1969)	0·929	−11·388	0
Storm (9 Aug 1969)	0·883	−8·204	1
BETTY (16 Aug 1972)	0·948	−20·343	1
JEAN (19 Jul 1974)	0·970	−12·075	1
BESS (11 Oct 1974)	0·913	−1·606	0
NINA (4 Aug 1975)	0·914	−12·793	0
BILLIE (9 Aug 1976)	0·929	−4·938	1
Storm (11 Aug 1976)	0·868	−16·490	1
Storm (16 Sep 1976)	0·951	−13·317	0
VERA (31 Jul 1977)	0·940	−14·608	0
Storm (15 Nov 1977)	0·982	−3·304	1
ANDY (29 Jul 1982)	0·971	−1·690	0
CECIL (9 Aug 1982)	0·987	−0·534	0
Storm (2 Jun 1984)	0·948	−9·182	0
FREDA (6 Aug 1984)	0·904	−13·781	1
GERALD (14 Aug 1984)	0·949	−8·842	0
BILL (18 Nov 1984)	0·997	−0·942	1
ALEX (27 Jul 1987)	0·868	−4·811	−1
LYNN (23 Oct 1987)	0·858	−18·392	−1
Storm (29 Sep 1988)	0·990	−5·180	2
SARAH (10 Sep 1989)	0·975	−3·022	2
OFELIA (22 Jun 1990)	0·971	−8·420	0
ABE (30 Aug 1990)	0·953	−12·878	1
Storm (1 Sep 1990)	0·948	−12·778	1
Storm (2 Sep 1990)	0·900	−8·274	1
Storm (22 Sep 1991)	0·946	−10·194	−2
NAT (29 Sep 1991)	0·997	−2·788	0
RUTH (28 Oct 1991)	0·990	−4·733	0
Storm (18 Jun 1994)	0·914	−9·681	1
DOUG (7 Aug 1994)	0·970	−4·953	1
GLADYS (1 Sep 1994)	0·927	−10·260	0
HERB (31 Jul 1996)	0·964	−6·855	0
ZANE (27 Sep 1996)	0·974	−12·873	0
CASS (29 Aug 1997)	0·964	−6·098	0

two of the calibrated rainfall–runoff events are plotted in Figures 3 and 4.

Regarding CE for model calibration, 36 calibrated events exceed 0·9 and the other four are near to the value of 0·9, as shown in Table II. With regard to EQ_p, all samples are smaller than 20%, except for one that is slightly over 20%. The ET_p values are all less than or equal to 2 h. The model calibration from the three evaluated criteria demonstrates that the calibrated parameters are adequately able to illustrate the situation of the researched watershed during urbanization.

Relationship between hydrological parameters and impervious surface

The relationship of the parameters and imperviousness can be analysed from the perspective of urban hydrology. By relying on this perspective, outlet hydrographs of the Wu-Tu watershed were simulated and used to indicate the possible urbanized effects on rainfall–runoff relationships. In that process, the hydrological uncertainty, such

DOI: 10.1002/hyp

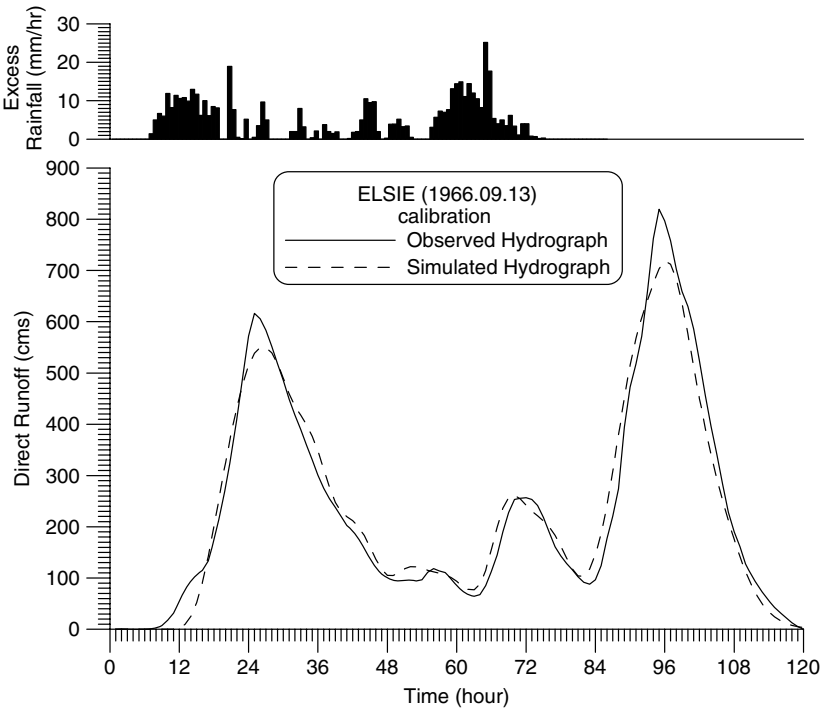

Figure 3. Calibration of observed and simulated hydrographs for ELSIE typhoon

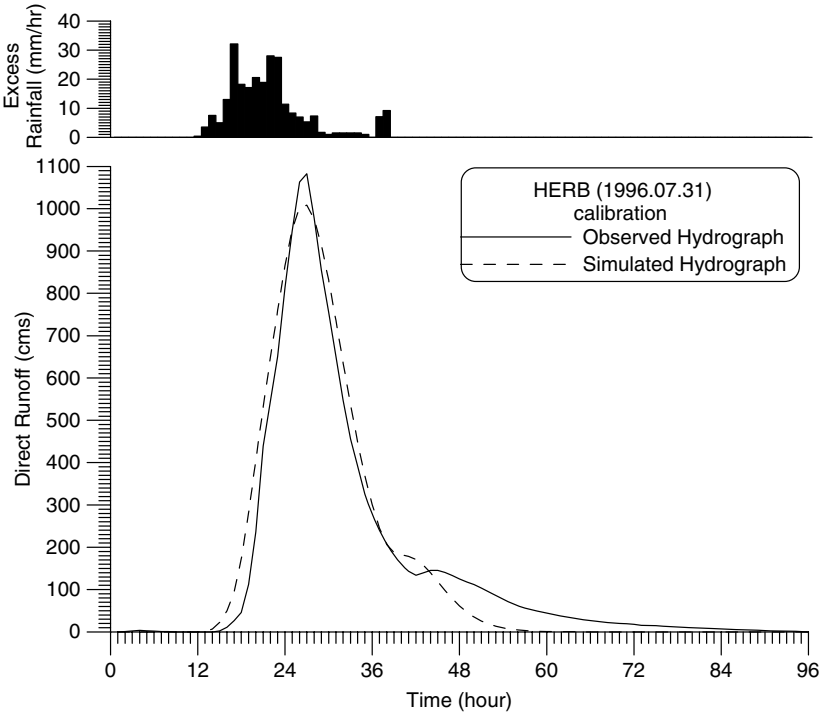

Figure 4. Calibration of observed and simulated hydrographs for HERB typhoon

as the influences of weather, antecedent moisture condition, or some uncontrollable factors, may cause irregular appearances of the calibrated parameters and thus affect the clarity of the results.

In order to prevent the above possibility, this study proposes an effective method to make any changing trends of the parameters clearer. The main procedure of the method uses a suitable interval for any variations of the local parameters and impervious areas, and these parameters and imperviousness located at that equivalent interval are viewed as having the same value and are averaged. By this method, a smoother/clearer urbanized behaviour can be easily observed on the researched watershed over the years. In this study, this method is called the optimal interval method.

The results of the calibrated parameters obtained through the optimal interval method are listed in Table III. From Table III, it is found that the dispersion of

DOI: 10.1002/hyp

Table III. Changes of parameters with impervious surfaces undergoing urbanization

Impervious area (%)	SCS CN	Nash	
		n	*k*
4.780	36·616	7·450	1·855
5.180	34·041	6·160	1·824
5.705	38·792	5·600	1·991
6.990	43·030	4·600	1·990
7.263	38·610	4·983	2·360
7.675	46·707	4·450	2·755
9.590	45·104	4·150	2·260
10.327	44·383	4·333	2·030
10.775	45·846	4·583	2·743
Mean	41·459	5·145	2·201
Standard deviation	4·539	1·079	0·355

parameter n is larger than parameter k, because the standard deviation of parameter n is 1·079 whereas k is 0·355. This result shows that the number of linear reservoirs is more responsive to impervious portions than the storage coefficient. Parameter n obviously decreases and parameter k varies slightly. Hence, the storage parameter k is considered as a fixed value; its value is an average of the parameter values of each interval listed in Table III and is equal to 2·201. In particular, the variation of parameter n should be provided with a continuous function. The power equation of regression was applied herein to fit the data of the parameters n in the second column of Table III. The fitting equation is expressed below and is shown in Figure 5:

$$n = 15{\cdot}75\mathrm{Im}^{-0{\cdot}57} \quad R^2 = 0{\cdot}78 \tag{17}$$

where n is the parameter of the hydrological model which represents the number of cascaded linear reservoirs and Im denotes the percentage of the impervious area over the upstream Wu-Tu watershed.

Variation in curve numbers with urbanization

The outlet discharge data came from hourly observations of streamflow of 40 rainfall–runoff events used for calibration. The hourly mean rainfall was the same value resulting form the block kriging method. Finally, the composite curve numbers CN were obtained from Equations (6)–(9) and the non-linear least squares method, which reflect significantly the hydrological and geomorphic statuses at that time.

The change in the curve number CN depending on its corresponding impervious area was treated with the same approach (the optimal interval method) as parameters n and k. Then, the power regression was fitted to the data representing the CN as a function of the imperviousness (Table III and Figure 6) and is expressed as below

$$\mathrm{CN} = 21{\cdot}80\mathrm{Im}^{0{\cdot}32} \quad R^2 = 0{\cdot}72 \tag{18}$$

where CN represents the composite value of the curve numbers.

Verification of established functional relationships

To test and verify the usability for the established relationships of parameters n and CN in urban areas, the remaining 10 events from 1998 to 2002 were chosen to examine the verifiability of these parameters. The baseflow was still assumed as a constant and the rainfall excesses of each event were estimated using the SCS method, in which the value of parameter CN was computed from Equation (18) with the relative annual imperviousness. The hydrological model with the fixed parameter k and its parameter n following the annual change of impervious covering (Equation (17)) was applied and convoluted to direct runoff. Table IV and Figures 7 and 8 present the verification. In Table IV, the values for the coefficient of efficiency of the verification model exceed 0·75, except for one event (LEKIMA, 25 Sep 2001), and the error of peak discharge is less than 25%, except for one event (RAMMASUN, 04 Jul 2002). The error in the arrival time of the peak of all events examined is 3 h or less, excluding the RAMMASUN typhoon.

Although the parameters and imperviousness have an incomplete correlation, the calibration and verification can still be supported by these regression equations (Equations (17) and (18)), which represent major trends of urbanization over the upstream Wu-Tu

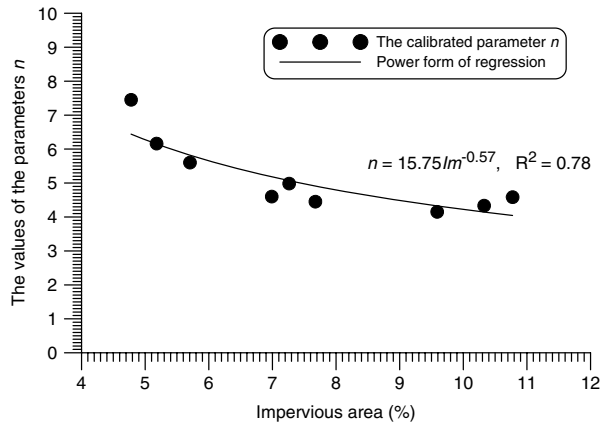

Figure 5. Decreased trend of parameter n with increased impervious areas

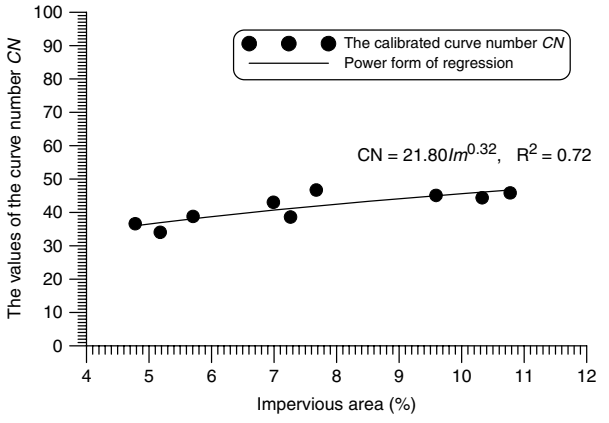

Figure 6. Change of the composite curve number with increased impervious areas

DOI: 10.1002/hyp

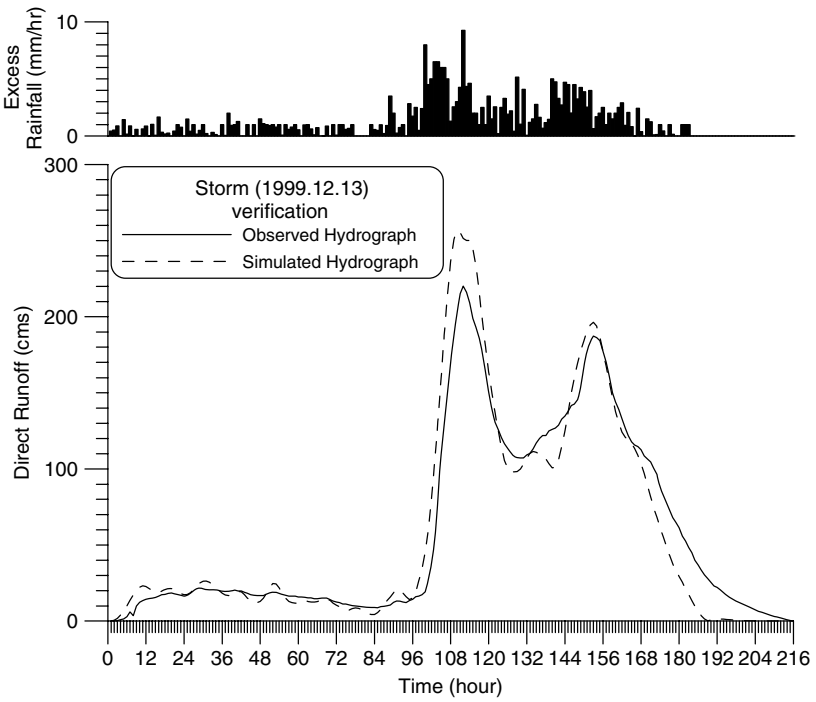

Figure 7. Verification of observed and simulated hydrographs for the 13 Dec 1999 storm

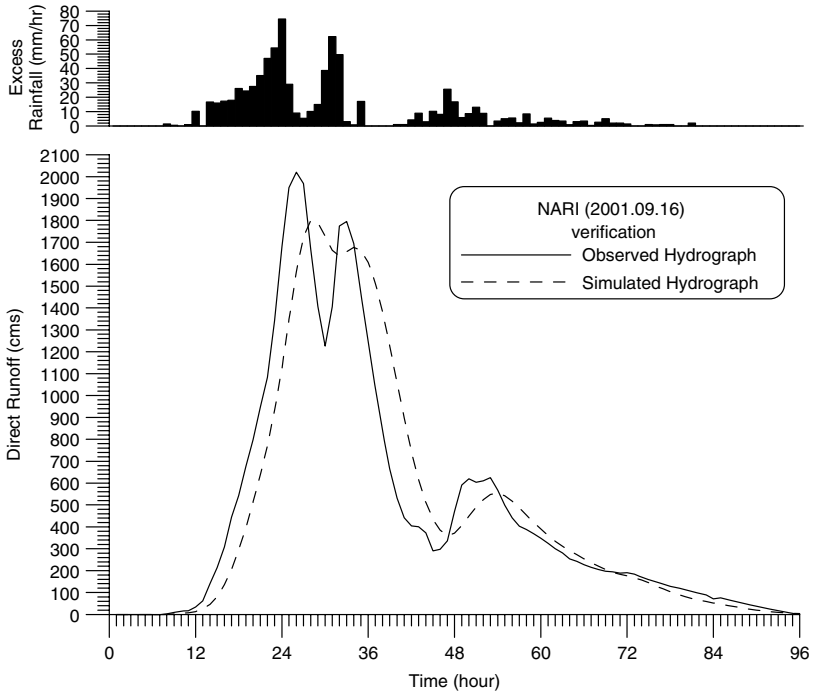

Figure 8. Verification of observed and simulated hydrographs for NARI typhoon

watershed. Consequently, these results show that imperviousness is the main influence of urbanization and, therefore, can be applied further to other relative applications.

Runoff characteristics of past and present flood hydrographs

The flood hydrograph is always concerned with water resources management, such as flood-control, inundation potential, and so on. Each independent storm certainly brings a different disaster; the causes and variations are complex and hard to understand clearly. This study employed a concept of probability distribution to simulate these storms while ignoring some unknown factors. Simulation modelling is considered to be the refined way of stormwater modelling.

This study adopted the alternating block method (Chow *et al.*, 1988) to structure the design storm of each rain-gauge from the IDF curve. The same duration of

DOI: 10.1002/hyp

Table IV. The verification of the selected rainfall-runoff events

Event name (date)	CE	EQ_p	ET_p
Storm (4 Oct 1998)	0·943	4·137	0
ZEB (15 Oct 1998)	0·941	5·356	1
Storm (13 Dec 1999)	0·915	16·492	−2
BILIS (22 Aug 2000)	0·787	2·901	2
BEBINCA (8 Nov 2000)	0·867	−7·691	2
Storm (13 Dec 2000)	0·955	−7·843	1
Storm (19 Dec 2000)	0·795	14·602	3
NARI (16 Sep 2001)	0·858	−10·970	2
LEKIMA (25 Sep 2001)	0·710	20·601	2
RAMMASUN (4 Jul 2002)	0·819	29·594	4

these design precipitation hyetographs is 48 h and the design return periods are 1·1, 2, 5, 10, 25, 50, 100, and 200 years. The mean design storm of the watershed studied is a linear combination based on the block kriging method, which was taken from the design precipitation hyetographs of three rain-gauges used in this study. The input of the rainfall–runoff model is the effective mean design storm, which was derived from the SCS method with its corresponding curve number and impervious surfaces (Equation (18)).

In general, the kernel function (IUH) of a watershed is denoted as a transformation relationship of excess rainfall into direct runoff. The kernel was determined herein by assuming that the value of parameter n is a power function of an impervious area as expressed in Equation (17), while parameter k is fixed at 2·201. Hence, the effective mean design storms can be convoluted to the design flood hydrograph. Design storm routings can be used to understand the changes of the surface runoff characteristics under various storms and land coverings; consequently, the design flood hydrograph of the return period of 200 years for 1966, 1976, 1986, 1996 and 2002 is plotted in Figure 9 and shows the effects of urbanization on the Wu-Tu watershed.

By using the combination of the design mean storm and the equations containing both parameters n and CN with their corresponding imperviousness, different shapes of flood hydrographs (Figure 9) can be created to observe the past and present hydrological status of the watershed. The results can illustrate the hydrological variation of the research watershed due to urbanization. The shape of the hydrographs has become more sharply pointed, with peaks shifted more forward due to increased impervious coverings, especially after 1986.

For further understanding of the changing degree of hydrological conditions, this study lists the time to peak and peak flow of flood hydrographs for eight return periods of the past natural status to the present urban status, as shown in Table V. It is found that the time to peak of the flood hydrographs for various storms diminishes as a result of increasing impervious coverings, decreasing approximately from 11 h to 6 h at different decrements. While peak discharge increases about 127, 266, 375, 440, 515, 564, 593, and 629 $m^3\ s^{-1}$, there are more increments of peak flow shown for the larger storms than for smaller storms. In Table V, a truth can be acknowledged that the peak of flood hydrographs of identical storms of present urbanization have larger peaks than those of the less-urbanized past; moreover, larger increments occur even more so with larger storms.

Changes for peak ratios from the natural status to the urban status

By taking into consideration that the future will continue to have increasing imperviousness, the values for the percentage of impervious surfaces were extended to 100%, although an impervious covering that would

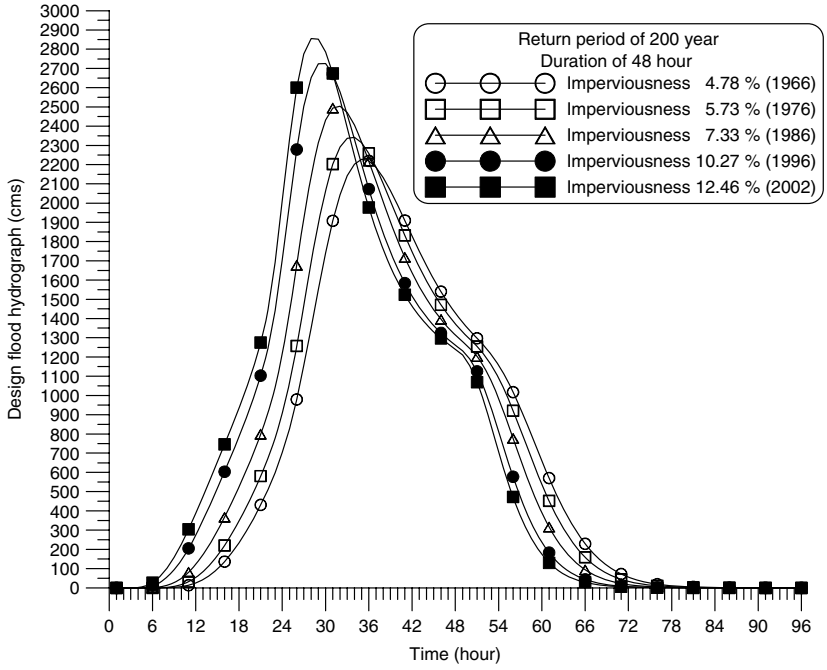

Figure 9. Shapes of flood hydrograph for return period of 200 years over the years

DOI: 10.1002/hyp

Table V. Changes of runoff characteristics for various design criteria of the natural status and urban status

Return period (years)	Time to peak (h)		Peak flow (m^3 s^{-1})	
	Natural status	Urban status	Natural status	Urban status
1.1	41	30	82·45	209·29
2	37	29	282·73	549·18
5	36	29	539·77	915·14
10	36	29	761·83	1201·56
25	36	29	1097·39	1612·19
50	36	29	1381·24	1944·86
100	35	29	1723·80	2317·23
200	34	28	2226·93	2856·18

occupy a whole watershed is an impossible occurrence. The flood hydrographs were simulated from the design storms with eight return periods and duration of 48 h by assuming that the growth of impervious paving will be from 4·78% to 100%. The ratios of the peaks for flood hydrographs of the urban status $Q_{p,urban}$ to that of the natural status $Q_{p,natural}$ were designed and are presented in Figure 10, in which the definition of a natural status is an impervious area that is equal to 4·78% (1966) and the urban status is larger than 4·78%, i.e. 4·79, 5·0, ..., 100%.

The design of the diagram for peak ratio (Figure 10) needs to be provided in order to get the peak discharge for specific imperviousness and return periods. For example, the percentage value of future impervious coverings is estimated by some trustworthy methods (e.g. Lazaro, 1979; Mather *et al*., 1998; Wilk and Hughes, 2002) and its value is assumed to be 40%. The ratio value in peak discharge of flood hydrographs for a return period of 200 years can be found directly in Figure 10, which is about 1·6 times the peak in its natural condition.

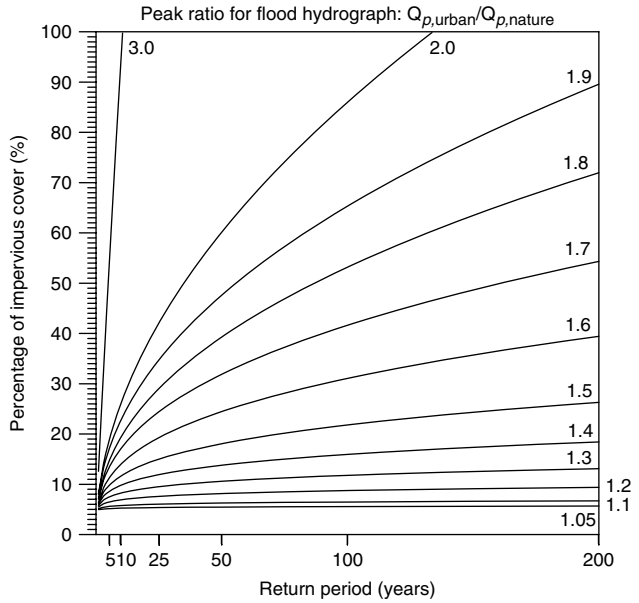

Figure 10. Increasing ratio of peak flow from the natural status to the urban status

Therefore, the peak flood for a return period of 200 years is 3563 m^3 s^{-1} because the peak discharge of the natural status is 2226·93 m^3 s^{-1}, as shown in Table V. This diagram can be a practical and beneficial help in water resources management and drainage engineering. Other similar diagrams for different durations of design storms can also be drawn up by following the procedure this study proposes.

CONCLUSIONS

This study successfully simulated the surface runoff derived from the use of simple models with significant parameters. The fine performances of the calibration based on the worst values for the three evaluation criteria are about 0·9 for CE, 20% for the error of peak discharge, and 2 h for the error of the time for peak to arrive. The block kriging and NLP methods can effectively help to obtain optimal parameters for representing the hydrological status of the research watershed. Certainly, the established relationships are satisfactorily verified from the results of the same evaluation methods; their most unfavourable evaluated values are 0·75 for CE, 25% for the error of peak discharge, and 3 h for the error of the time for peak to arrive. It is confirmed herein that the relationships between imperviousness and parameters can desirably assist in observing urbanized effects on the study area.

The parameter n clearly decreases from a value of 7·45 to 4·58, while imperviousness increases from 4·78% to 10·78%. The values of parameter CN range from 36·62 to 45·85. The advantages of this study procedure lies in realizing that the alterations of the time to peak and peak flow within the process are able to transform rainfall into runoff. However, these analytical results demonstrate that the flood hydrographs inevitably vary with urbanization, thus possibly causing greater disaster. The evaluation of potential flood disasters can be easily accomplished by analysing the trend of the parameters of the Nash IUH and the SCS models.

The simulated results of design storms for eight return periods and duration of 48 h indicate that the time to peak of the flood hydrographs is diminished as a result of increasing impervious coverings, between 11 h and 6 h in different decrements for various storms, while the peak flow increases from 127, 266, 375, 440, 515, 564, 593, to 629 m^3 s^{-1} for different storm intensities. There is a greater increment of peaks for larger storms than for smaller storms. The design of a diagram with the peak ratio expressed as a function of a return period and with impervious percentages can greatly assist engineers in applications of water resources.

REFERENCES

Agirre U, Goñi M, López JJ, Gimena FN. 2005. Application of a unit hydrograph based on subwatershed division and comparison with Nash's instantaneous unit hydrograph. *Catena* **64**: 321–332.

DOI: 10.1002/hyp

Beven K. 1989. Changing ideals in hydrology: the case of physically-based models. *Journal of Hydrology* **105**: 157–172.

Bonta JV, Amerman CR, Harlukowicz TJ, Dick WA. 1997. Impact of coal surface mining on three Ohio watersheds—surface-water hydrology. *Journal of the American Water Resources Association* **33**: 907–917.

Changnon D, Fox D, Bork S. 1996. Differences in warm-season, rainstorm-generated stormflows for northeastern Illinois urbanized basins. *Water Resources Bulletin* **32**: 1307–1317.

Chen RS, Pi LC, Huang YH. 2003. Analysis of rainfall–runoff relation in paddy fields by diffusive tank model. *Hydrological Processes* **17**: 2541–2553.

Cheng S-J, Wang R-Y. 2002. An approach for evaluating the hydrological effects of urbanization and its application. *Hydrological Processes* **16**: 1403–1418.

Chiles JP, Delfiner P. 1999. *Geostatistics: Modeling Spatial Uncertainty*. Wiley: New York.

Chow VT, Maidment DR, Mays LW. 1988. *Applied Hydrology*. McGraw-Hill: New York.

Clarke RT. 1973. A review of some mathematical models used in hydrology, with observations on their calibration and use. *Journal of Hydrology* **19**: 1–20.

Driver NE, Troutman BM. 1989. Regression models for estimating urban storm-runoff quality and quantity in the United States. *Journal of Hydrology* **109**: 221–236.

Duan Q, Gupta VK, Sorooshian S. 1993. Shuffled complex evolution approach for effective and efficient global minimization. *Journal of Optimization Theory Application* **76**: 501–521.

Ferguson BK, Suckling PW. 1990. Changing rainfall–runoff relationships in the urbanizing Peachtree Creek watershed, Atlanta, Georgia. *Water Resources Bulletin* **26**: 313–322.

Franchini M, O'Connell PE. 1996. An analysis of the dynamic component of the geomorphologic instantaneous unit hydrograph. *Journal of Hydrology* **175**: 407–428.

Goovaerts P. 2000. Geostatistical approaches for incorporating elevation into the spatial interpolation of rainfall. *Journal of Hydrology* **228**: 113–129.

Gremillion P, Gonyeau A, Wanielista M. 2000. Application of alternative hydrograph separation models to detect changes in flow paths in a watershed undergoing urban development. *Hydrological Processes* **14**: 1485–1501.

Hannah DM, Gurnell AM. 2001. A Conceptual, linear reservoir runoff model to investigate melt season changes in cirque glacier hydrology. *Journal of Hydrology* **246**: 123–141.

Hollis GE. 1975. The effect of urbanization on floods of different recurrence interval. *Water Resources Research* **11**: 431–435.

Hsieh L-S, Wang R-Y. 1999. A semi-distributed parallel-type linear reservoir rainfall–runoff model and its application in Taiwan. *Hydrological Processes* **13**: 1247–1268.

Jin CX. 1992. A deterministic gamma-type geomorphologic instantaneous unit hydrograph based on path types. *Water Resources Research* **28**: 479–486.

Kang IS, Park JI, Singh VP. 1998. Effect of urbanization on runoff characteristics of the On-Cheon Stream watershed in Pusan, Korea. *Hydrological Processes* **12**: 351–363.

Krug WR. 1996. Simulation of temporal changes in rainfall-runoff characteristics, Coon Creek basin, Wisconsin. *Water Resources Bulletin* **32**: 745–752.

Lazaro TR. 1979. *Urban Hydrology*. Ann Arbor Science Publishers: Ann Arbor, MI.

Lebel T, Bastin G. 1985. Variogram identification by the mean squared interpolation error method with application to hydrologic field. *Journal of Hydrology* **77**: 31–56.

Lebel T, Bastin G, Obled C, Creutin JD. 1987. On the accuracy of areal rainfall estimation: a case study. *Water Resources Research* **23**: 2123–2134.

Lee YH, Singh VP. 2005. Tank model for sediment yield. *Water Resources Management* **19**: 349–362.

Legates DR, McCabe Jr GJ. 1999. Evaluating the use of 'goodness-of-fit' measures in hydrologic and hydroclimatic model validation. *Water Resource Research* **35**: 233–241.

Leopold LB. 1991. Lag times for small drainage basins. *Catena* **18**: 157–171.

Loganathan GV, Delleur JW. 1984. Effects of urbanization on frequencies of overflows and pollutant loading from storm sewer overflows: a derived distribution approach. *Water Resources Research* **20**: 857–865.

Marsalek J, Sztruhar D. 1994. Urban drainage: review of contemporary approaches. *Water Science and Technology* **29**: 1–10.

Mather AS, Needle CL, Fairbairn J. 1998. The human derivers of global land cover change: the case of forests. *Hydrological Processes* **12**: 1983–1994.

Matheron G. 1971. *The Theory of Regionalized Variables and Its Application*. Cahiers du Centre de Morphologic Mathematique, Ecole des Mines: Fountainbleau, France.

Melone F, Corradini C, Singh VP. 1998. Simulation of the direct runoff hydrograph at basin outlet. *Hydrological Processes* **12**: 769–779.

Moon J, Kim J-H, Yoo C. 2004. Storm-coverage effect on dynamic flood-frequency analysis: empirical data analysis. *Hydrological Processes* **18**: 159–178.

Moramarco T, Melone F, Singh VP. 2005. Assessment of flooding in urbanized ungauged basins: a case study in the upper Tiber area, Italy. *Hydrological Processes* **19**: 1909–1924.

Moscrip AL, Montgomery DR. 1997. Urbanization, flood frequency, and salmon abundance in Puget lowland streams. *Journal of the American Water Resources Association* **33**: 1289–1297.

Nash JE. 1958. The form of the instantaneous unit hydrograph. In *General Assembly of Toronto, 3–14 September 1957, Volume III, Surface Water, Prevision, Evaporation*. *IAHS Publication* No. 45. IAHS Press: Wallingford; 114–121.

Nash JE, Sutcliffe JV. 1970. River flow forecasting through conceptual models: 1. A discussion of principles. *Journal of Hydrology* **10**: 282–290.

Nayak PC, Sudheer KP, Ramasastri KS. 2005. Fuzzy computing based rainfall–runoff model for real time flood forecasting. *Hydrological Processes* **19**: 955–968.

Rodriguez F, Andrieu H, Creutin J-D. 2003. Surface runoff in urban catchments: morphological identification of unit hydrographs from urban databanks. *Journal of Hydrology* **283**: 146–168.

Sala M, Inbar M. 1992. Some hydrologic effects of urbanization in Catalan rivers. *Catena* **19**: 363–378.

Simmons DL, Reynolds RJ. 1982. Effects of urbanization on base flow of selected south-shore streams, Long Island, New York. *Water Resources Bulletin* **18**: 797–805.

Singh RB. 1998. Land use/cover changes, extreme events and ecohydrological response in the Himalayan region. *Hydrological Processes* **12**: 2043–2055.

Syed KH, Goodrich DC, Myers DE, Sorooshian S. 2003. Spatial characteristics of thunderstorm rainfall fields and their relation to runoff. *Journal of Hydrology* **271**: 1–21.

Tsihrintzis VA, Hamid R. 1997. Urban stormwater quantity/quality modeling using the SCS method and empirical equations. *Journal of the American Water Resources Association* **33**: 163–176.

Wackernagel H. 1998. *Multivariate Geostatistics*. Springer-Verlag: Berlin.

Wilk J, Hughes DA. 2002. Simulating the impacts of land-use and climate change on water resource availability for a large south Indian catchment. *Hydrological Sciences* **47**: 19–30.

Wong TSW, Li Y. 1999. Theoretical assessment of changes in design flood peak of an overland plane for two opposing urbanization sequences. *Hydrological Processes* **13**: 1629–1647.

Yue S, Hashino M. 2000. Unit hydrographs to model quick and slow runoff components of streamflow. *Journal of Hydrology* **227**: 195–206.

DOI: 10.1002/hyp